

Bistability of a hydrogen defect with a vibrational mode at 3326 cm⁻¹ in ZnOF. Herklotz and I. Chaplygin
*Technische Universität Dresden, 01062 Dresden, Germany*E. V. Lavrov
*Technische Universität Dresden, 01062 Dresden, Germany and Tomsk State University, 634050 Tomsk, Russia*A. Neiman, R. J. Reeves, and M. W. Allen
MacDiarmid Institute for Advanced Materials and Nanotechnology, University of Canterbury, Christchurch 8014, New Zealand

(Received 14 January 2019; published 14 March 2019; corrected 8 April 2019)

Results from illumination-sensitive infrared absorption and photocurrent spectroscopy measurements on the hydrogen defect in ZnO characterized by a local vibrational mode with a frequency of 3326 cm⁻¹ are reported. It is shown that photoexcitation with $\hbar\omega \geq 2.7$ eV results in two new axial oriented O-H stretch vibrational modes at 3170 and 3589 cm⁻¹, which appear at the expense of the previously reported azimuthal oriented 3326- and 3358-cm⁻¹ modes. We propose a tentative configurational-coordinate energy diagram of the defect and discuss its microscopic origin.

DOI: [10.1103/PhysRevB.99.115203](https://doi.org/10.1103/PhysRevB.99.115203)**I. INTRODUCTION**

The influence of impurities, native defects, and their complexes on the optical and electrical properties of ZnO has been investigated and debated for decades. Hydrogen is an omnipresent impurity in ZnO that can be unintentionally incorporated into the material during crystal growth and/or device processing. Interest in hydrogen comes from its high mobility and strong impact on the electrical behavior of ZnO, which results from its ability to form shallow donor states and/or passivate acceptors [1–12]. Unambiguous spectroscopic identification of hydrogen-related complexes is therefore of key importance for gaining control over the parameters of ZnO-based semiconductor devices.

Interstitial hydrogen in ZnO occurs in the bond-centered configuration, H_{BC}, which acts as an effective-mass-like shallow donor with an ionization energy of 53 meV [3,12]. H_{BC} comprises a strong *c*-oriented single dative O-H bond characterized by a local vibrational mode (LVM) with a frequency of 3611 cm⁻¹ (10 K) [13]. Interstitial hydrogen is highly mobile at room temperature and readily gets trapped by other defects or/and forms electrically neutral hydrogen molecule H₂ with another H_{BC} in the course of a few weeks [12,14,15].

The subject of the present work is an electrically active hydrogen-related defect comprised of a single O-H bond aligned approximately perpendicular to the *c* axis of a crystal and characterized by a 3326-cm⁻¹ LVM at 10 K. The defect was originally associated with an isolated hydrogen located at the antibonding site of the ZnO lattice (H_{AB}) [9]. Later on, other microscopic models were put forward to account for an origin of the 3326-cm⁻¹ line, none of them, however, being fully consistent with available experimental data [15–18]. Depending on the hydrogen isotope we label this defect XH/XD.

The electrical activity of the XH complex remains controversial. A correlation between the intensity of the 3326-cm⁻¹

line and free carrier concentration was taken as a strong indication that the defect is a shallow donor [19,20]. Later on, it was shown that the XH behavior can be also understood in a framework of a deep acceptor model, whereby the free carrier concentration actually correlates with the intensity of the 3611-cm⁻¹ line of H_{BC} rather than with that of the 3326-cm⁻¹ line [15,20].

It was also demonstrated that illumination of ZnO samples with red light ($\hbar\omega \approx 1.9$ eV) at liquid helium temperatures transforms XH from the ground to a metastable state characterized by a LVM with a frequency of 3358 cm⁻¹ [15]. In both states the O-H bond was found to lie in the basal plane of the ZnO crystal. The ground and the metastable configuration were assigned to the (*n*) and (*n* + 1) charge states of the same complex, respectively.

In the present paper we report on two new metastable configurations of the XH complex which appear as a result of photoexcitation by light with $\hbar\omega \geq 2.7$ eV at helium temperatures. The O-H bond in both configurations is aligned parallel to the *c* axis of the ZnO crystal. A configurational-coordinate energy diagram of XH is proposed to explain all known experimental data. The microscopic origin of the complex is discussed.

II. EXPERIMENTAL DETAILS

ZnO samples used in the present study were commercial melt-grown *a*- and *c*-cut ZnO wafers purchased from Cermet, Inc. and had dimensions of about 5 × 5 × 0.4 mm³. Hydrogen and/or deuterium were introduced into the samples via thermal treatments (anneals) in closed quartz ampules filled with H₂, D₂, or a mixture of H₂ and D₂ gas. The treatments were performed at 730 °C for 1 h and terminated by quenching the ampules to room temperature in water.

For photoconductivity measurements the ZnO samples were first etched with orthophosphoric acid for 2 min at room temperature. Ohmic contacts with an area of about $2 \times 1 \text{ mm}^2$ were generated by scratching a mixture of an In-Ga alloy onto the sample surface. Contacts were located on the illuminated face of the samples.

Fourier transform infrared (FTIR) absorbance and photoconductivity spectra were recorded using a Bomem DA3.01 Fourier spectrometer equipped with a globar light source and a KBr beam splitter. Absorbance and photoconductivity measurements were performed with a spectral resolution of 0.5 and 1 cm^{-1} , respectively, with the temperature of the samples stabilized within 1 K in the range of 7–13 K. Unless noted otherwise, unpolarized light was used with the wave vector k directed perpendicular to the c axis of the samples. Polarized light was produced by a wire grid polarizer with a KRS-5 substrate. Absorption spectra were corrected for the absorption lines of residual CO_2 in the spectrometer using reference spectra.

Illumination of the samples was performed with unpolarized light supplied by commercial high-power LEDs with nominal peak emissions at either 375 nm ('UV'), 395 nm ('UV 2'), 460 nm ('blue'), 530 nm ('green'), 640 nm ('red'), or 850 nm ('NIR'). Unless noted otherwise, illumination took place at $\sim 10 \text{ K}$ and was continued until no further change in absorption spectra was observable. The radiant flux density was in the range of $20\text{--}200 \text{ Wm}^{-2}$. Spectra shown were recorded after illumination had been switched off.

III. RESULTS

A. General properties of the IR lines

Figure 1 shows sections of IR absorption spectra obtained for ZnO samples treated in H_2 (top) and D_2 (bottom) gas. The black spectra were recorded at 10 K without additional illumination ('reference'), whereas the red and blue ones were obtained after subsequent illumination by LEDs with wavelengths of 640 nm and 460 nm, respectively. Only the ground state modes of the XH and XD defects at 3326 and 2471 cm^{-1} , respectively, are seen in the reference spectra. The signals due to the LVMs of H_{BC} and D_{BC} donors are also observed (not shown). They are insensitive to the illumination and will not be further discussed here.

The red illumination results in the appearance of two lines positioned at 3358 and 2489 cm^{-1} at the expense of the main signals at 3326 (XH) and 2471 cm^{-1} (XD), respectively. For the sake of clarity, only the deuterium modes are shown. Virtually full interconversion takes place within less than one minute. The same behavior was reported in Ref. [15] and was associated with an $n \rightarrow n+1$ charge transition of the XH defect. In accordance with that study, intensities of the photoinduced modes are a factor of about 7 (hydrogen) and 4.8 (deuterium) weaker than the original modes. The photoinduced state is metastable and persists up to about 70 K. We label the ground and the metastable states of the XH defect as XH_A and XH_B , respectively.

As can be seen from the figure, illumination with the blue LED results in a significantly different picture. The XH_A/XD_A signals also become strongly suppressed compared

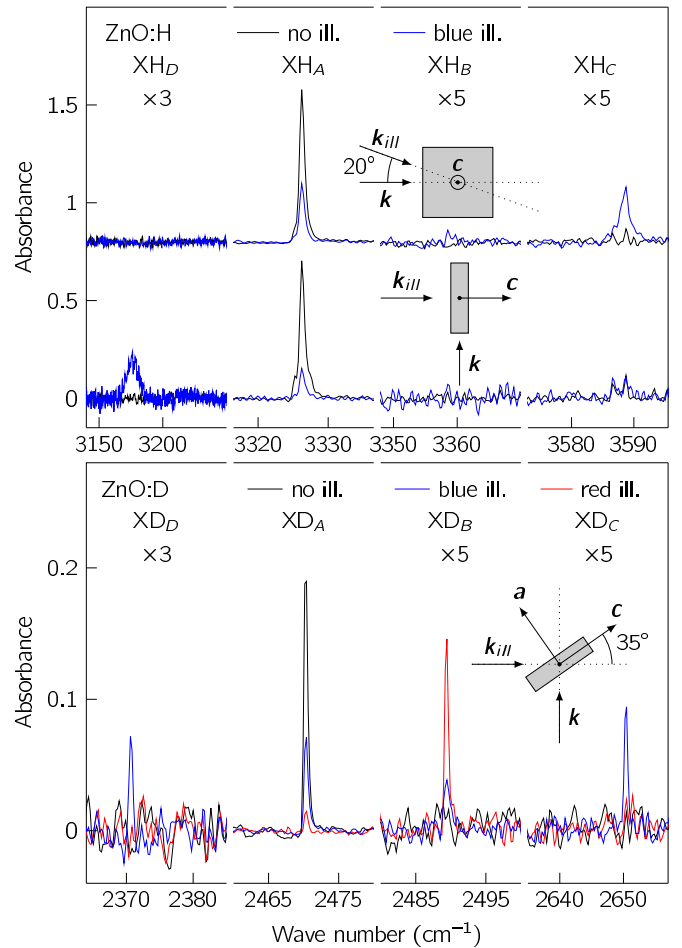


FIG. 1. Sections of IR absorption spectra obtained at 10 K for a hydrogenated (top panel) and deuterated (bottom panel) melt-grown ZnO samples subjected to illumination from high-power LEDs with different wavelengths: black—reference (no illumination), red—640 nm, blue—460 nm. Spectra in the top panel are vertically offset for clarity. Insets show the measurement/illumination geometries.

to the preilluminated state, but conversion to the XH_B/XD_B configurations does not occur. Instead, two new lines appear in the spectra: at ~ 3174 and 3589 cm^{-1} in the case of ZnO:H and at 2371 and 2651 cm^{-1} in the case of ZnO:D. The frequency ratios of each pair, $3174/2371 = 1.339$ and $3589/2651 = 1.354$, are close to the value expected for a harmonic oscillator consisting of a hydrogen/deuterium atom bound to oxygen. Based on this we conclude that all photoinduced lines are due to the local vibrational modes of the O-H/O-D species as well.

When the blue illumination is switched off, the intensities of the photoinduced signals remain constant at $T \leq 10 \text{ K}$ for at least one hour. Moreover, a weighted sum of the signal intensities from the A and B states together with the new lines remains constant, independently of whether the illumination is switched on or off and which illumination duration or geometry has been applied. The inverse of the weighting coefficients is proportional to the oscillator strengths f of each LVM, that is, correlates the LVM specific absorption coefficients of f are gathered in Table I. These values are, within the accuracy of our measurement, independent of the particular

TABLE I. LVM frequencies (in cm^{-1}) and corresponding oscillator strengths f of the XH defect. Oscillator strengths are given relative to the A configuration.

Configuration	XH		XD	
	ω	f	ω	f
A	3326	1	2471	1
B	3358	0.13 ± 0.01	2489	0.22 ± 0.02
C	3589	0.22 ± 0.06	2651	0.26 ± 0.04
D	3174	1.61 ± 0.18	2371	1.69 ± 0.13

sample, which strongly indicates that the observed vibrational modes originate from different states of the same complex. Throughout this work we will label the defect states associated with the new absorption lines at 3589 and $\sim 3174 \text{ cm}^{-1}$ XH_C and XH_D , respectively. As evident from the figure, the FWHM (full width at half maximum) of LVMs due to the XD complex is significantly less compared to those due to XH. Because of this, in the following discussion, we will concentrate on the results obtained for the deuterium counterpart of the defect without, however, loss of generality.

The relative intensities of the photoinduced lines strongly depend not only on the wavelength of the secondary illumination but also on the measurement/illumination geometry which are shown as insets in Fig. 1. Importantly, the $A \rightarrow C$ conversion was found to be much faster compared to the $A \rightarrow D$ one: The C state saturates within less than a minute, whereas the transition to the D state is not completed even after several hours of blue LED illumination. From the entirety of our data we conclude that the different populations of the C and D configurations observed in Fig. 1 can be explained by these differences in the conversion rate. However, an influence of other experimental parameters, like, e.g., the orientation of the incident secondary illumination or sample thickness cannot be completely excluded.

Figure 2 reveals polarized properties of the LVMs due to the XD complex. Surprisingly, IR absorption spectra

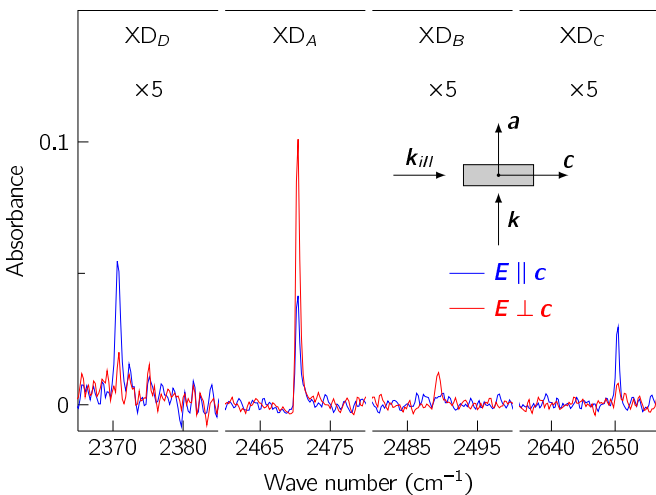


FIG. 2. Polarized IR absorption spectra of a deuterated ZnO sample subjected to 2 h of blue LED illumination. The spectra were taken at 10 K.

demonstrate that the O-D bond of the XD_C and XD_D configurations is aligned along the c axis of the ZnO lattice. In contrast, the O-D (O-H) bond in both A and B states is aligned perpendicular to c (see also Refs. [9,15]). We conclude from here that transitions from A and B to the C and D configurations of the defect and vice versa are accompanied by a rearrangement of its hydrogen bond.

B. Wavelength dependence of the photoinduced conversion

The effect of illumination on the states of XH and their interconversion was investigated for different illumination wavelengths. First, we discuss the results obtained from measurements where the sample was cooled down from room temperature to $\sim 10 \text{ K}$ in the dark and then exposed to light with a specified wavelength. In this case a predominant $\text{XH}_A \rightarrow \text{XH}_B$ conversion is achieved by the light with the wavelength of 640 nm (red spectrum in Fig. 1). Illumination by NIR (850 nm) or green (530 nm) light does not result in any observable changes of the ground state. For the wavelengths shorter than 530 nm, i.e., 460, 395, or 375 nm the additional excitation paths to the XH_C or XH_D states emerge.

We now turn to experiments where the samples were exposed to light from the NIR LED after conversion into the B configuration had been accomplished. Exemplary spectra obtained for the XD complex in a course of such a ‘two-stage’ illumination procedure are shown in the top panel of Fig. 3. The black and red spectra were recorded before and after the red light illumination. As one can see, such a procedure results in a full conversion of the ground XD_A to the metastable XD_B state.

Interestingly, subsequent illumination with NIR light for 30 s (orange spectra) results in an appearance of the XD_C configuration. At the same time the ground XD_A state partially regains its intensity. Prolonged exposure to the NIR light for 1220 s leads to a continual decrease in the XD_B and XD_C LVM intensities and a recovery of the XD_A state. The dynamics of the back conversion is shown in the lower panel of Fig. 3. These findings demonstrate that the C configuration of the XH defect can be populated by: (i) illumination by light with a wavelength shorter than 530 nm or (ii) a ‘two-step’ procedure consisting of subsequent illumination by red and near IR light. Our experimental data also indicate that a $C \rightarrow A$ transition is induced by the NIR illumination.

C. Thermal stability

The photoinduced conversion from the ground state of XH to the metastable configurations is completely reversible by annealing the sample at elevated temperatures. Figure 4 demonstrates the process for the XD complex. The black spectrum (labeled ‘ref.’) was recorded at 10 K after a sample was cooled down in darkness. Subsequently, it was illuminated for 3 h by a blue LED to populate the metastable states of XD. The corresponding spectrum is given in blue. Further on, the spectra were recorded at 10 K after each step in a series of 5 min anneals at gradually increasing temperature. Interestingly, annealing at $\sim 48 \text{ K}$ results in a full conversion from the XD_C to the XD_B configuration, while the intensities of the ground XD_A state and the metastable XD_D configuration

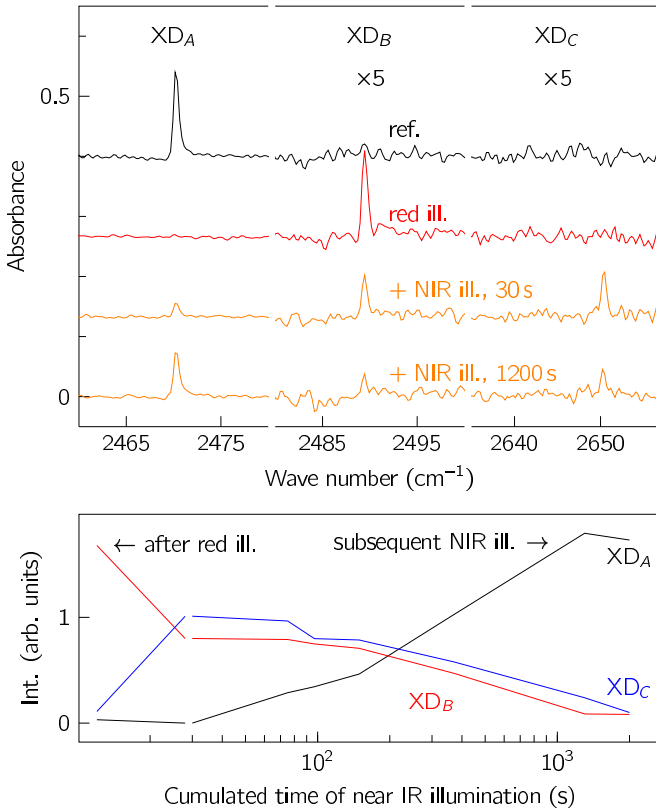


FIG. 3. Top: IR absorption spectra recorded on a deuterated ZnO sample after consecutive steps of a two-stage illumination experiment: black—reference (no illumination); red 5 min illumination with a red LED; orange 30 and 1200 s illumination from a NIR LED. Spectra are offset vertically for clarity. Bottom: LVM intensities of the XD_A , XD_B , and XD_C signals as a function of the cumulated illumination time with the NIR LED after conversion to the XD_B defect configuration has been established by illumination with the red LED. Illumination has been switched off during absorption measurements.

remain constant. Further annealing at 90 K transforms the XD_B to XD_A configuration. Earlier, this reconversion process was found to be thermally activated with an activation energy of about 220 meV [15]. The intensity of the XD_D mode remains constant at this annealing step. Finally, annealing the sample at temperatures above 160 K results in complete recovery of the ground XD_A state.

D. Photoconductivity

Recently, photoconductivity (PC) was shown to be an efficient method to probe vibrational excitations of defects in semiconductors [21–24]. The basic principle of this technique is an interaction of a vibrational mode with the continuum of electronic states in the conduction/valence band resulting in the appearance of Fano resonances in the photoconductivity spectra (see Fig. 1 in Ref. [23]). Compared with conventional IR absorption, PC-based vibrational mode spectroscopy has three major advantages:

- (i) exceptional selectivity and sensitivity [23,24],
- (ii) possibility to detect local vibrational modes even in strongly absorbing and/or reflecting spectroscopic regions [21], and

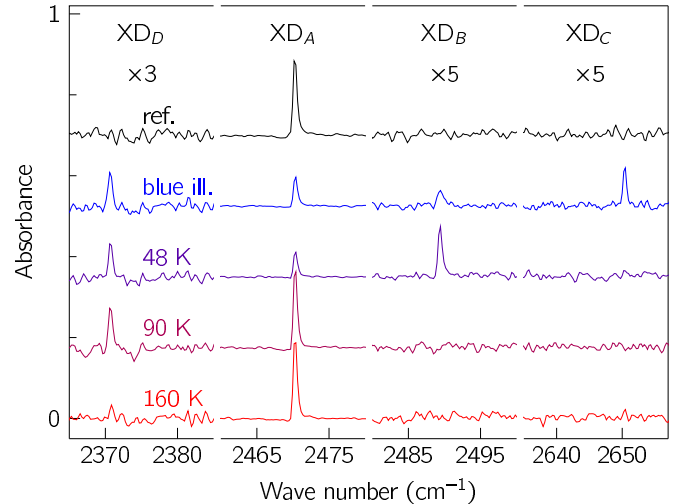


FIG. 4. IR absorption spectra recorded at 10 K on a deuterated ZnO sample before (black) and after (blue) illumination with the blue LED. Subsequent spectra were obtained after annealing for 5 min at indicated temperatures (see text for details). Spectra are offset vertically for clarity.

(iii) the sign of the Fano resonance allows us to gain direct insight into the electrical activity of defects resulting in the LVM [23,25].

The method has been successfully applied to probe H_{BC} and H_O in ZnO [21–23], interstitial oxygen in ultrathin Si films [24], and interstitial hydrogen in rutile TiO_2 [22,23]. Here, this method is applied to gain insight into electrical activity of the different configurations of XH.

Figure 5 shows sections of photoconductivity (top panel) and absorption (bottom panel) spectra taken for two different D_2 -treated ZnO samples labeled ① and ②, which were subjected to the secondary illumination supplied by the red and blue LED, respectively. As expected, only the mode at 2471 cm^{-1} due to the ground XD_A state is observed in the absorption spectra of both samples without secondary illumination. Unexpectedly, the same mode appears in the PC spectra as a *positive* Fano resonance, which strongly indicates that the defect must have an electronic level above $E_c - 0.3\text{ eV}$ [25].

Notably, the PC peak intensity resulting from XD_A in sample ① appears to be stronger than that detected in sample ②. This can be understood if one takes into account that both the shape and intensity of Fano resonances due to LVMs critically depend not only on the nature of the defects but also on its concentration and the presence of other donors/acceptors (for details see Ref. [25]).

As discussed in the previous sections, a full conversion from XD_A to XD_B takes place if the sample is illuminated with the red light, whereas transition to XD_D dominates upon illumination with the blue LED. This can be seen from the IR absorption spectra presented in the bottom panel of Fig. 5. As expected, the positive Fano resonance due to XD_A disappears from the photoconductivity spectra after the defect is converted from the ground state to its metastable configurations. Importantly, the XD_D state of the defect with a vibrational mode at 2371 cm^{-1} manifests itself as a *negative*

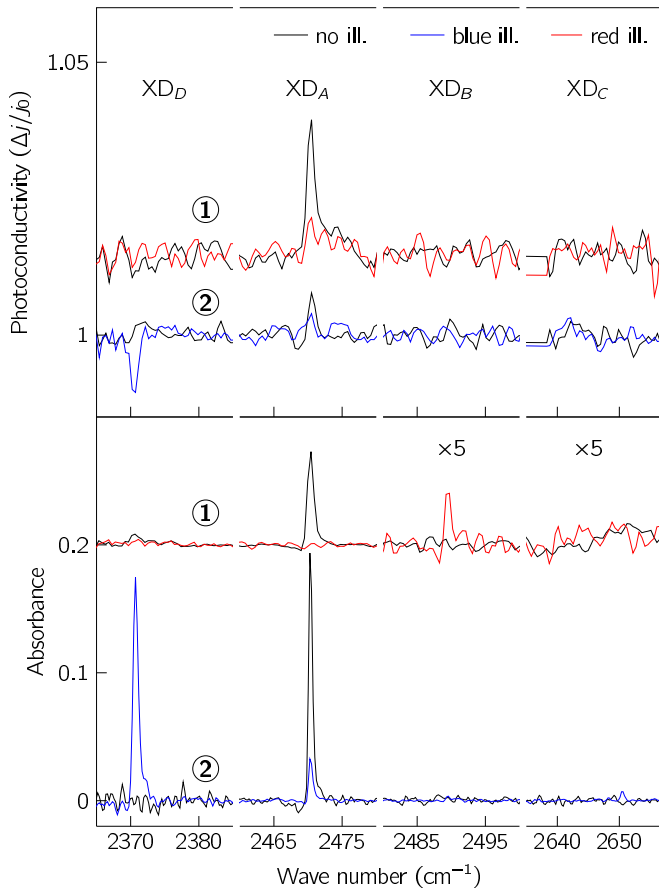


FIG. 5. Sections of photoconductivity (top panel) and absorption spectra (bottom panel) obtained on two different deuterated ZnO samples (labeled ① and ②) recorded before and after illumination from LEDs with different wavelength: black—reference (before illumination), red—640 nm (‘red’), blue—460 nm (‘blue’). Spectra are vertically offset for clarity.

Fano resonance in the photoconductivity spectrum. This finding strongly indicates that the D state has no level above $E_c - 0.3$ eV.

No signal related to the XD_B configuration is detected in the PC spectra. The weakness of this line and the substantial noise in the spectra could presumably explain why the latter signal escapes observation.

IV. DISCUSSION

A. Earlier studies

Light-induced effects of the XH complex in ZnO were first considered by Shi *et al.* [20] and Nickel. [26] Shi *et al.* have found that illumination of samples by white light from a tungsten lamp reduces the intensity of the 3326-cm^{-1} line. Similar results were obtained by Nickel who employed a blue LED with a wavelength of 450 nm. None of the photoinduced modes discussed here or a complementary change in the intensity of other hydrogen-related IR absorption lines have been reported by both groups. Later on, Herklotz *et al.* have observed the 3358-cm^{-1} line which appears at the expense of the 3326-cm^{-1} mode as a result of illumination with red 633 nm light from a He-Ne laser or the broadband quartz lamp

of the Fourier spectrometer [15]. The C and D configurations of XH have escaped observation so far. This fact can be explained by a combination of the following circumstances.

(i) All earlier IR absorption studies were conducted on c -cut ZnO wafers with the incident light polarized perpendicular to the c axis (see Ref. [26]). Such a measurement geometry makes observation of the O-H bonds aligned parallel to c basically impossible.

(ii) The LVM of XH_C occurs in a spectroscopic region strongly disturbed by absorption lines of residual water vapor in the spectrometer.

(iii) The photoinduced transitions between the XH configurations are strongly dependent on the spectrum of the incident light.

(iv) The $A \rightarrow D$ transformation requires a relatively high power and/or long illumination time.

B. The $V_{Zn}H$ model

A number of models were proposed to account for the defect giving rise to the 3326-cm^{-1} IR absorption line. First, we discuss a Zn vacancy passivated by a single hydrogen atom, $V_{Zn}H$ [15,16]. The zinc vacancy is a native double acceptor in ZnO [27–29], acting as a compensating center in n -type material. Several first-principles calculations conclusively predict that the vacancies are further stabilized by binding one or more hydrogen atoms to form vacancy-hydrogen complexes, $V_{Zn}H_n$ [27,29–31]. In this process, the hydrogen atoms passivate the double-acceptor states of V_{Zn} by terminating the dangling O $2p$ bonds. Theory predicts that the vacancy-hydrogen complexes, once spontaneously formed during growth or subsequent processing of ZnO, are relatively stable due to the high dissociation energies.

Most spectroscopic evidence for defects of the $V_{Zn}H_n$ series exists for the zinc vacancy decorated by two hydrogen atoms, $V_{Zn}H_2$ [13,32,33]. This electrically neutral defect has two different configurations: a ground state comprising two inequivalent O-H bonds aligned parallel and perpendicular to the c axis of the crystal with LVMs of 3312.2 and 3349.6 cm^{-1} [13], respectively, and a metastable state that consists of two equivalent O-H bonds oriented perpendicular to the c axis with LVMs of 3329.0 and 3348.4 cm^{-1} [33]. The $V_{Zn}H_2$ complex anneals out at about 500 °C [13].

The body of experimental data on the $V_{Zn}H$ and $V_{Zn}H_3$ centers in ZnO is scarce and less conclusive. Recently, absorption lines at 3303 and 3321 cm^{-1} observed in hydrogenated ZnO crystals have been tentatively assigned to LVMs of the $V_{Zn}H_3$ complex [34]. A further mode at 3327 cm^{-1} has been attributed to $V_{Zn}H$ [35]. This assignment, however, needs to be validated by further studies.

First principles studies by Lyons *et al.* [27] and Frodason *et al.* [29] agree that the trapping of one or two H atoms at the Zn vacancy to form $V_{Zn}H$ or $V_{Zn}H_2$ is highly energetically favorable. Once spontaneously formed during crystal growth or processing of ZnO, these complexes are unlikely to dissociate. Frodason *et al.* [29] and Karazhanov *et al.* [31] also suggest that further trapping of hydrogen to form $V_{Zn}H_3$ may take place whereby the relative amounts of the $V_{Zn}H_n$ complexes are strongly dependent on the concentration ratio of H_i and V_{Zn} as well as the detailed sample history.

From an experimental point of view, $V_{Zn}H$, $V_{Zn}H_2$, and $V_{Zn}H_3$ should be easily observable via IR absorption on their O-H local vibrational modes. As mentioned earlier, the identification of a defect with two LVMs at 3312 and 3349 cm^{-1} as $V_{Zn}H_2$ stands on solid ground [13,32,33]. Though less unambiguous, the center with three equivalent hydrogen atoms characterized by LVMs at 3303 and 3321 cm^{-1} has been attributed to the planar configuration of $V_{Zn}H_3$ [34]. The latter two complexes, along with XH, have been simultaneously observed in a course of an annealing series performed on hydrogenated vapor-phase grown ZnO (see Fig. 4 in Ref. [34]).

A common property of all these defects is a configurational bistability. $V_{Zn}H_2$ has a metastable planar structural configuration, comprising two equivalent O-H bonds [33]. The energy difference between the ground and the metastable state was found to be about 75 meV, whereas the activation energy of the hydrogen motion within the Zn vacancy is ~ 0.96 eV. Further, weak sidebands observed with the main LVMs of the above-mentioned triple-hydrogen complex have been attributed to a metastable nonplanar defect configuration [34]. Metastability of these centers and XH is consistent with the $V_{Zn}H_n$ model since first principles calculations predict that differences in the total energy between axial and basal configurations of this series of complexes are marginal [27,29,30,36]. For example, energies of the axial and azimuthal configurations of $V_{Zn}H$ differ by less than 50 meV.

The calculations by Lyons *et al.* and Frodason *et al.* also address optical transitions and electrical levels of $V_{Zn}H$ [27,29]. The complex was found to have four different charge states across the band gap of ZnO (from -1 to $+2$), where all possible thermodynamic charge-state transition levels, $(-/0)$, $(0/+)$, and $(+/2+)$, occur in the lower half of the band gap. In *n*-type ZnO, $V_{Zn}H$ therefore occurs as a singly negatively charged deep compensating acceptor. Electron emission of $V_{Zn}H^-$ to the conduction band by photons gives rise to a broad absorption band with a lower threshold of 2.09 eV, which is in rough agreement with our experimental value of $\sim 1.7 \pm 0.25$ eV determined for the optical $A \rightarrow B$ transition.

Though it would be tempting to assign the XH complex to $V_{Zn}H$, in view of our findings, this model meets serious difficulties. First of all, our photoconductivity spectra strongly indicate that XH has a level located above $E_c - 0.3$ eV. This finding is consistent with the shallow donor behavior of XH suggested by the work of Ref. [19]. Unless the defect has a $(2 - /-)$ level in the upper part of the band gap it cannot be $V_{Zn}H$ since all theoretical calculations predict that the highest $(-/0)$ level of $V_{Zn}H$ is located in the lower part of the band gap. Secondly, our data also reveal that illumination with blue light results in reorientation of the O-H bond from perpendicular to the parallel alignment relative to the *c* axis. In the framework of the $V_{Zn}H$ model this would imply that hydrogen should break up the O-H bond and move to the nearby oxygen atom. The energy budget of this jump, however, is expected to be too high to take place at 10 K. For comparison, activation energy of hydrogen motion within the $V_{Zn}H_2$ complex is about 0.96 eV [33]. Finally, all theoretical calculations performed for the $V_{Zn}H_n$ complexes so far did not find a vibrational mode with a frequency as high

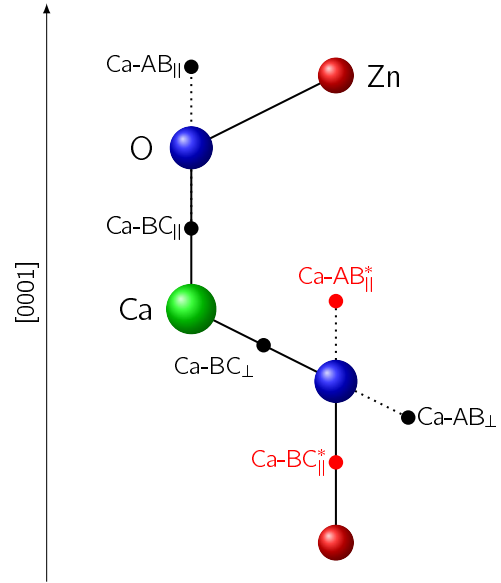


FIG. 6. Schematics in the $(11\bar{2}0)$ plane of the hydrogen sites near a Ca impurity. The black sites mark those considered theoretically in Ref. [18].

as 3589 cm^{-1} . Though we still do not rule out completely the $V_{Zn}H$ model of the XH defect, we admit that it cannot satisfactorily account for all available experimental findings.

C. The CaH model

Secondary-ion mass spectroscopy and delayed gamma neutron activation analysis revealed that Cermet ZnO contains approximately 4×10^{16} cm^{-3} of Ca [17]. Since the 3326 - cm^{-1} line was found to be the strongest in this material, it was suggested that Ca is the missing constituent of the XH complex. First principles theory finds that substitutional Ca at the Zn site with H bound to the nearby O with the O-H bond aligned perpendicular to the *c* axis (site Ca-AB_\perp in Fig. 6) could account for the stability and LVM frequency of the XH complex [18]. Earlier, it was pointed out that due to the isoelectronic nature of Ca with respect to Zn, the CaH complex is expected to act as a shallow donor [15]. Our photoconductivity spectra presented in Fig. 5 clearly reveal that XH must have a level above $E_c - 0.3$ eV, which is consistent with the suggestion about the electrical activity of CaH. In view of this finding as well as our results on the secondary illumination it is worth revisiting the CaH model.

The experimental observations presented in this work conclusively demonstrate that the XH complex possesses four different states with distinctively different orientational properties: The *A* and *B* states contain O-H bonds aligned perpendicular to the *c* axis of the ZnO crystal, whereas the O-H bonds of the other two states, *C* and *D*, are aligned parallel to the *c* axis. Unexpectedly, such a transformation occurs at 10 K. This leads us to the conclusion that independent of the configuration, hydrogen remains bound to the same oxygen atom. The CaH model seems to be consistent with this suggestion. The red spots labeled Ca-AB_\parallel^* and Ca-BC_\parallel^* in

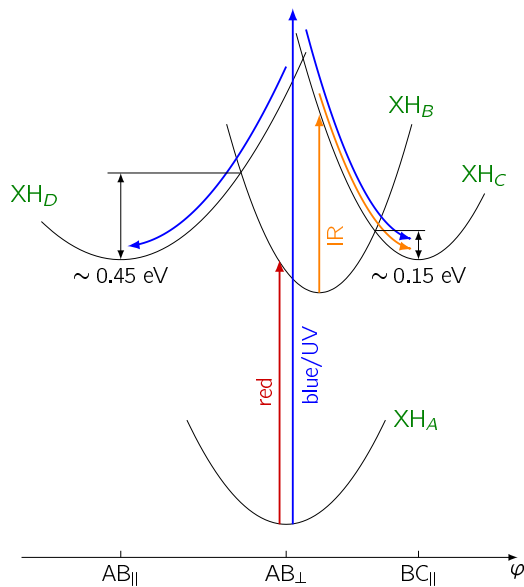


FIG. 7. Configurational-coordinate energy diagram of the XH complex.

Fig. 6 together with the ground state Ca-AB_⊥ would be the likely sites for hydrogen to occupy.

Figure 7 presents a tentative configuration-coordinate energy diagram of the XH complex. The ground *A* state corresponds to the neutral charge state of the defect with hydrogen positioned at the Ca-AB_⊥ site. Illumination with the red light transforms the *A* configuration into the positively charged state *B* leaving orientation of the O-H bond unchanged. Subsequent illumination with NIR light would transform the *B* state into *C* corresponding to the Ca-BC_{||}* site. Secondary illumination with the blue light would transform the *A* state into *C* and *D*, the latter being the Ca-AB_⊥* site. The reason why the Ca-BC_{||}* site is associated with the *C* state rather than with Ca-AB_⊥* is a frequency of its LVM of 3589 cm⁻¹. Theory finds that hydrogen located at the bond-centered sites of ZnO has LVMs with significantly higher frequencies compared to the antibonding positions [3].

The thermal stability of XH presented in Fig. 4 let us estimate energy barriers separating the *C* and *D* states from *B* (E_{CB} and E_{DB} , respectively). Transition temperatures of 48 and 160 K suggests that they are $E_{CB} \approx 0.15$ and $E_{DB} \approx 0.45$ eV. Earlier it was established that the back $B \rightarrow A$ transition is also thermally activated with the time constant of $\tau = \tau_0 \exp(E_{BA}/kT)$ with $\tau_0 \approx 3.4 \times 10^{-15}$ s and $E_{BA} = 220$ meV [15]. Since $E_{CB} < E_{BA} < E_{DB}$ this explains why the back $D \rightarrow B$ transition was never observed, whereas the $C \rightarrow B$ one is easily detected (see Fig. 4).

The position of the donor (0/+) level of XH can be estimated independently from the temperature dependence of the LVM intensity of XH_A. Since the integrated intensity of an IR absorption line depends on temperature as $\coth(\hbar\omega/2kT)$ [37], temperature should have no effect on the intensity on any LVM from 10 to 300 K. This implies that the intensity of the 3326-cm⁻¹ line as a function of temperature will directly reveal the amount of XH in the neutral charge state. At room temperature (RT) the 3326-cm⁻¹ mode is shifted

to a frequency of ~ 3336 cm⁻¹ [38]. It turned out that in our samples the LVM intensity of the *A* configuration at RT is half as strong compared to the low temperature value. An exact determination of the $E_c - E_{XH}$ level is, however, hardly possible since there are too many unknown parameters affecting the outcome of the fit, e.g., concentrations of XH, amount and type of other donors (assuming that XH is a donor), concentration of compensating acceptors, etc. Still, the fact that only half of XH becomes ionized at RT implies that the defect cannot be a standard shallow donor.

This is not the only flaw in the CaH model. Since the *A* and *B* configurations represent different charge states of the same defect, the energy difference between the two configurations should match the position of the $E_c - E_{XH}$ level in the band gap of ZnO, i.e., $E_B - E_A < 0.3$ eV. This is about an order of magnitude less than the energy quantum of light employed for the secondary illumination. We find it puzzling, because no effects due to the secondary illumination were found for the LVM of interstitial hydrogen H_{BC} acting as a shallow donor in ZnO.

To verify whether Ca is involved into the XH defect formation we undertook an attempt to introduce Ca ions into a vapor-phase grown sample of ZnO [39] which does not reveal the 3326-cm⁻¹ line upon hydrogenation. The sample was boiled in a water solution of calcium hydroxide to cover its surface with a thin layer of Ca(OH)₂. Subsequently the sample was annealed for 1 hour at 725 °C in a sealed quartz ampule filled with a mixture of hydrogen and deuterium. The only new absorption lines appearing after this treatment were those of bond-centered hydrogen and deuterium, and a pronounced broad peak centered at 3650 cm⁻¹, which we attribute to the A_{2u} fundamental OH stretching mode of Ca(OH)₂ [40]. The deviation from the reported value (3644 cm⁻¹) is possibly due to lattice mismatch with that of bulk calcium hydroxide or the lower temperature of our measurement. The obtained results imply that calcium hydroxide neither decomposes nor diffuses into the ZnO crystals at the applied temperature. Thus the issue of calcium involvement into formation of the XH defect remains unresolved.

Finally, we note that it is possible that additional configurations of XH might have escaped observation in the present study. This particularly applies to possible configurations of XH which have either low configurational transformation rates or LVM's with low absorption strength and, thus, easily result in a failure to detect LVMs due to low signal-to-noise ratio. EPR measurements on the XH complex as well as further theoretical calculations are called for to unveil the nature of the XH defect.

V. SUMMARY

The hydrogen defect in ZnO with a local vibrational mode at 3326 cm⁻¹ is studied by a combination of illumination-sensitive infrared absorption and photocurrent spectroscopy. It is shown that the defect possesses at least four different charge configurations. Two of these, the ground state with the 3326-cm⁻¹ mode and the previously observed metastable state with a LVM at 3358 cm⁻¹, have an azimuthal oriented O-H bond configuration. Conversion to and reconversion from the metastable state is achieved by illumination with red light

($\hbar\omega \approx 2$ eV) and annealing at about 70 K, respectively. Two further previously unreported metastable states with axial oriented O-H bonds and LVMs at 3589 and ~ 3174 cm^{-1} appear upon photoexcitation with $\hbar\omega \geq 2.7$ eV. Back conversion to the azimuthal defect configuration occurs upon annealing at about 40 and 160 K, respectively.

ACKNOWLEDGMENTS

This work was funded by the Deutsche Forschungsgemeinschaft (Grant No. LA 1397/10). E.V.L. acknowledges the support by the Tomsk State University competitiveness improvement program (Project No. 8.2.22.2018).

-
- [1] E. Mollwo, *Z. Phys.* **138**, 478 (1954).
 [2] D. G. Thomas and J. J. Lander, *J. Chem. Phys.* **25**, 1136 (1956).
 [3] C. G. Van de Walle, *Phys. Rev. Lett.* **85**, 1012 (2000).
 [4] A. Janotti and C. G. Van de Walle, *Nat. Mater.* **6**, 44 (2007).
 [5] S. F. J. Cox, E. A. Davis, S. P. Cottrell, P. J. C. King, J. S. Lord, J. M. Gil, H. V. Alberto, R. C. Vilão, J. Pirotto Duarte, N. Ayres de Campos *et al.*, *Phys. Rev. Lett.* **86**, 2601 (2001).
 [6] K. Shimomura, K. Nishiyama, and R. Kadono, *Phys. Rev. Lett.* **89**, 255505 (2002).
 [7] D. M. Hofmann, A. Hofstaetter, F. Leiter, H. J. Zhou, F. Henecker, B. K. Meyer, S. B. Orlinskii, J. Schmidt, and P. G. Baranov, *Phys. Rev. Lett.* **88**, 045504 (2002).
 [8] B. K. Meyer, H. Alves, D. M. Hofmann, W. Kriegseis, D. Forster, F. Bertram, J. Christen, A. Hoffmann, M. Straßburg, M. Dworzak *et al.*, *Phys. Status Solidi B* **241**, 231 (2004).
 [9] M. D. McCluskey, S. J. Jokela, K. K. Zhuravlev, P. J. Simpson, and K. G. Lynn, *Appl. Phys. Lett.* **81**, 3807 (2002).
 [10] C. H. Seager and S. M. Myers, *J. Appl. Phys.* **94**, 2888 (2003).
 [11] E. V. Lavrov, F. Börrnert, and J. Weber, *Phys. Rev. B* **71**, 035205 (2005).
 [12] E. V. Lavrov, F. Herklotz, and J. Weber, *Phys. Rev. B* **79**, 165210 (2009).
 [13] E. V. Lavrov, J. Weber, F. Börrnert, C. G. Van de Walle, and R. Helbig, *Phys. Rev. B* **66**, 165205 (2002).
 [14] E. V. Lavrov, F. Herklotz, and J. Weber, *Phys. Rev. Lett.* **102**, 185502 (2009).
 [15] F. Herklotz, E. V. Lavrov, V. I. Kolkovskiy, J. Weber, and M. Stavola, *Phys. Rev. B* **82**, 115206 (2010).
 [16] E. V. Lavrov, F. Börrnert, and J. Weber, *Physica B* **401–402**, 366 (2007).
 [17] M. D. McCluskey and S. J. Jokela, *Physica B* **401–402**, 355 (2007).
 [18] X.-B. Li, S. Limpijumng, W. Q. Tian, H.-B. Sun, and S. B. Zhang, *Phys. Rev. B* **78**, 113203 (2008).
 [19] S. J. Jokela and M. D. McCluskey, *Phys. Rev. B* **72**, 113201 (2005).
 [20] G. A. Shi, M. Stavola, S. J. Pearton, M. Thieme, E. V. Lavrov, and J. Weber, *Phys. Rev. B* **72**, 195211 (2005).
 [21] S. G. Koch, E. V. Lavrov, and J. Weber, *Phys. Rev. Lett.* **108**, 165501 (2012).
 [22] E. V. Lavrov, F. Herklotz, and J. Weber, *Semicond. Sci. Technol.* **30**, 024004 (2015).
 [23] E. V. Lavrov, T. Mchedlidze, and F. Herklotz, *J. Appl. Phys.* **120**, 055703 (2016).
 [24] E. V. Lavrov, I. Chaplygin, and T. Mchedlidze, *Appl. Phys. Lett.* **110**, 132102 (2017).
 [25] F. Herklotz, I. Chaplygin, and E. V. Lavrov, *J. Appl. Phys.* **124**, 025704 (2018).
 [26] N. H. Nickel, *Phys. Status Solidi B* **243**, R51 (2006).
 [27] J. L. Lyons, J. B. Varley, D. Steiauf, A. Janotti, and C. G. Van de Walle, *J. Appl. Phys.* **122**, 035704 (2017).
 [28] Y. K. Frodason, K. M. Johansen, T. S. Bjørheim, B. G. Svensson, and A. Alkauskas, *Phys. Rev. B* **95**, 094105 (2017).
 [29] Y. K. Frodason, K. M. Johansen, T. S. Bjørheim, B. G. Svensson, and A. Alkauskas, *Phys. Rev. B* **97**, 104109 (2018).
 [30] M. G. Wardle, J. P. Goss, and P. R. Briddon, *Phys. Rev. B* **72**, 155108 (2005).
 [31] S. Z. Karazhanov, E. S. Marstein, and A. Holt, *J. Appl. Phys.* **105**, 033712 (2009).
 [32] E. V. Lavrov and J. Weber, *Phys. Rev. B* **73**, 035208 (2006).
 [33] D. Bastin, E. V. Lavrov, and J. Weber, *Phys. Rev. B* **83**, 195210 (2011).
 [34] F. Herklotz, A. Hupfer, K. M. Johansen, B. G. Svensson, S. G. Koch, and E. V. Lavrov, *Phys. Rev. B* **92**, 155203 (2015).
 [35] C. D. Corolewski, N. S. Parmar, K. G. Lynn, and M. D. McCluskey, *J. Appl. Phys.* **120**, 035703 (2016).
 [36] J. Bang and K. J. Chang, *J. Korean Phys. Soc.* **55**, 98 (2009).
 [37] B. N. J. Persson and R. Ryberg, *Phys. Rev. B* **32**, 3586 (1985).
 [38] M. McCluskey, S. Jokela, and W. H. Oo, *Physica B: Condensed Matter* **376–377**, 690 (2006).
 [39] R. Helbig, *J. Cryst. Growth* **15**, 25 (1972).
 [40] O. Oehler and H. H. Günthard, *J. Chem. Phys.* **48**, 2036 (1968).

Correction: The wave-number units were presented incorrectly during the production cycle and have been fixed.